Peer-reviewed version available at Sensors 2018, 18, 2528; doi:10.3390/s18082528

Article

Pendulum-type hetero-core fiber optic accelerometer for low-frequency vibration monitoring

Hiroshi Yamazaki [1,*], Ichiro Kurose [1], Michiko Nishiyama [2], and Kazuhiro Watanabe [2]

[1] Department of Information Systems Science, Faculty of Science and Engineering, SOKA university, 1-236 Tangi-machi, Hachioji, Tokyo 192-8577, Japan
[2] Department of Science and Engineering for Sustainable Innovation, Faculty of Science and Engineering, SOKA university, 1-236 Tangi-machi, Hachioji, Tokyo 192-8577, Japan; {mnishiya, kazuhiro}@soka.ac.jp
* Correspondence: hyamazaki@soka.ac.jp; Tel.: +81-042-691-9400

Abstract: In this paper, a novel pendulum-type accelerometer based on hetero-core fiber optics has been proposed for structural health monitoring targeting large-scale civil infrastructures. Vibration measurement is a non-destructive method for diagnosing the failure of structures by assessing natural frequencies and other vibration patterns. The hetero-core fiber optic sensor utilized in the proposed accelerometer can serve as a displacement sensor with robustness to temperature changes in addition to immunity to electromagnetic interference and chemical corrosions. Thus the hetero-core sensor inside the accelerometer measures applied acceleration by detecting the rotation of an internal pendulum. A series of experiments showed that the hetero-core fiber sensor linearly responded to the rotation angle of the pendulum ranging within ±5°, and furthermore the proposed accelerometer could reproduce the waveform of input vibration in a frequency band of several Hz order.

Keywords: structural health monitoring; fiber optic sensor; accelerometer; hetero-core; low-frequency vibration measurement

1. Introduction

For preventing serious disasters caused by civil infrastructures collapsed, the existence of structural damage and any other faults in infrastructures have to be early and accurately detected, in spite of uncountable infrastructures and the inadequate number of inspectors. The process of implementing fault diagnosis strategy is referred to as structural health monitoring (SHM), in which the failure in a structure is automatically observed by monitoring, data processing, and health evaluation systems [1].

As one of SHM techniques, fault diagnosis based on vibration monitoring was widely known as a non-destructive sensing and analysis scheme for global fault diagnosis and has been studied so far in the literature [2-5]. Typically, a decrease in stiffness of the structure is observed in a natural frequency getting lower than expected value. In contrast, the frequency higher than expected implies that the structure was supported stiffer than expected.

There have been a lot of studies researched for analyzing the faults in infrastructures from vibration information. For instance, Soman et al. employed several stiffness indices based on modal frequency, displacement and strain for quantifying the degree of structural health by use of a multi-metric measurement system [6]. Moreover, a practical non-destructive bridge condition assessment was also examined on an actual bridge using accelerometers in combination with cable tension sensors, anemometers and thermistors [7]. However, when considering practical usages in actual infrastructures, the SHM system should be robust to ambient noise, temperature changes and corrosions in harsh measurement environments [8].

With the development of vibration monitoring methodology, a number of sensing devices have also been proposed aiming at SHM based on electric-based sensors based on piezoelectric, capacitive, and [9-13]. However, it is necessary for the sensor devices to be highly robust to electromagnetic interference and severe temperature changes in order to monitor civil infrastructures for long term in harsh environments, which is always exposed to changes in weather, or sometimes water leakage and lightning damages. In comparison, fiber optic sensors were known as an alternative sensing technology to electric sensors for SHM because of their remarkable merits. Fiber optic sensors are non-electrical and passive devices, immune to electromagnetic interference and chemical corrosions, and have the ability of remote sensing, thereby those of which makes them suited to outdoor long-term smart sensing [14].

There have been a variety of fiber optic sensors developed for smart structures by use of Brillouin scattering [15, 16], fiber Bragg grating (FBG) [17-24], and optical interferometer [25, 26]. Minardo et al. introduced distributed fiber optic temperature and strain sensors using Brillouin optical time-domain analysis (BOTDA) into railway infrastructures and succeeded to dynamically monitor strain distribution due to train passage [15]. Moreover, a considerable number of fiber Bragg grating (FBG) sensors have also been proposed for detecting strain in structure by embedding sensors themselves [17-19], and they can perform as accelerometers by means of sensing the deformation of on an oscillated cantilever beam [20-22]. A fiber optic accelerometer based on Fabry-Perot interference were also investigated [25]. This accelerometer detects vibration in a range up to some hundreds Hz in such a way to measure the flexure of an optical fiber cantilever beam by Fabry-Perot interference.

In this paper, we have proposed a novel accelerometer based on a hetero-core fiber optic sensor for natural vibration monitoring on large-scale infrastructures. Hetero-core fiber optic sensors consist of two single-mode fibers fusion-spliced with different core diameters to obtain high sensitivity to macro-bending on the processed fiber line [27]. Compared to conventional fiber optic sensors, the hetero-core fiber sensors have some attractive features such as a cost-effective measurement scheme by use of a light emitting diode (LED) and a photo diode (PD), and temperature independency on sensor responses [28].

The scope of this study is to realize a pendulum-type accelerometer targeting low-frequency natural vibration on large-scale infrastructures, in which an embedded hetero-core sensor detects the rotation position of an internal pendulum. The movement of the pendulum was subjected to a combination of a weight and springs equipped with the pendulum so that they dominantly determined the resonance characteristics of the proposed accelerometer. On the other hand, it was so far demonstrated that the hetero-core sensor was able to measure displacement with high linearity by a conversion mechanism to transform displacement to macro-bending [29], thereby the rotation of pendulum can be detected in such a way that the hetero-core optical fiber measured the displacement on a given point on the pendulum. A series of experiments were conducted to confirm that the hetero-core optical fiber inside the accelerometer measures the rotation of internal pendulum with a good linearity. In addition, it was revealed that the accelerometer performed well in low-frequency vibration measurement by tuning the sensitivity and frequency response characteristics depending on dynamic parameters of the pendulum.

2. Sensor principle

As shown in Figure 1, a hetero-core fiber optic sensor proposed in this paper is composed of a short single mode (SM) fiber segment called a hetero-core portion, inserted by fusion splicing into an SM fiber transmission line. The core diameters of the hetero-core portion and the transmission line are 5 μm and 9 μm, respectively, and the length of the hetero-core portion is about 1-2 mm. It was previously confirmed that light transmitted through the core partially leaks into a cladding layer at a boundary between the transmission fiber and the hetero-core portion, and the degree of light leakage increases with a bending radius of the hetero-core portion [27].

Preprints (www.preprints.org) | NOT PEER-REVIEWED | Posted: 21 June 2018 doi:10.20944/preprints201806.0335.v1

Peer-reviewed version available at Sensors 2018, 18, 2528; doi:10.3390/s18082528

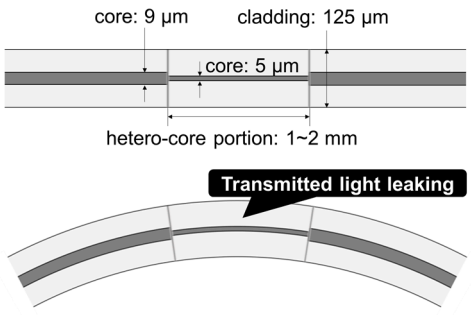

Figure 1. Schematics of a hetero-core fiber optic sensor.

A displacement sensor based on hetero-core fiber optics has already been reported [29] by employing the conversion mechanism from displacement to bending, as illustrated in Figure 2(a). The hetero-core optical fiber is clamped across the hetero-core portion by a pair of fiber clampers, one of which is set to move and the other is fixed. When the displacement of the clampers d increases, the optical loss of the sensor was linearly increased as the increment of bending radius on the hetero-core portion, as shown in Figure 2(b). The accuracy of the sensor to the displacement was less than 0.1 %FS so that the hetero-core fiber optic sensor can be employed as a highly-accurate displacement sensor.

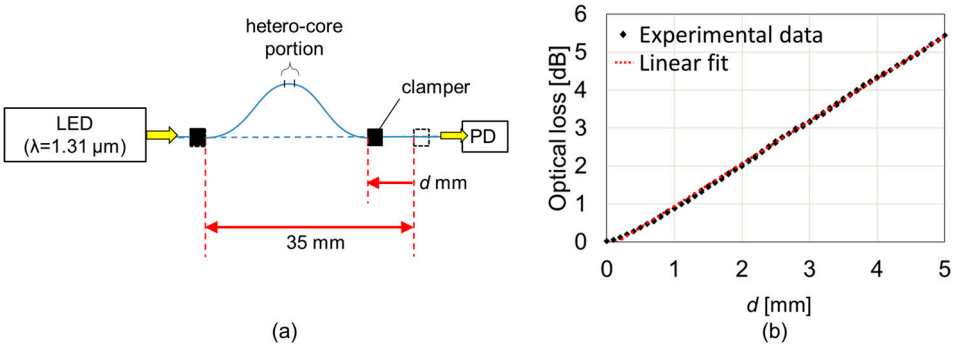

Figure 2. Sensing principle of a hetero-core fiber optic displacement sensor: (a) experimental setup and (b) optical loss response to applied displacement.

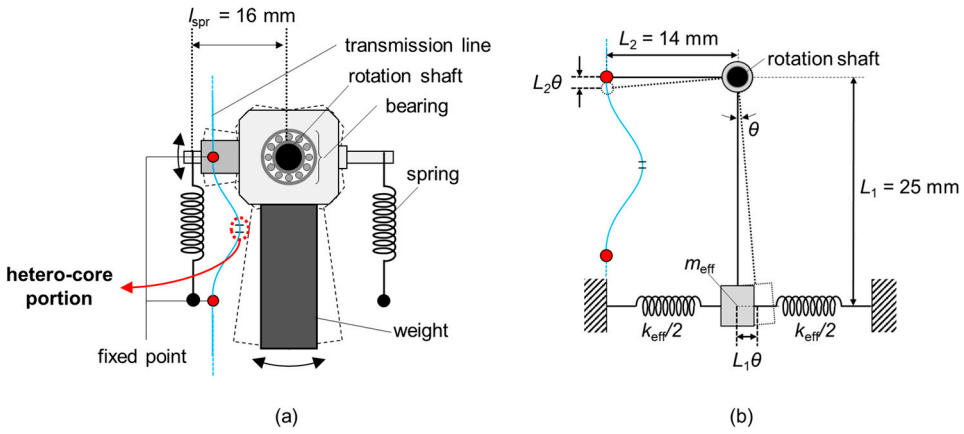

Figure 3. (a) Appearance and (b) schematics of a pendulum-type accelerometer with a hetero-core fiber optic sensor.

Figure 3 illustrates a schematic drawing of the proposed pendulum-type accelerometer based on hetero-core fiber optics. As shown in Figure 3(a), an internal pendulum built in the accelerometer equips a weight and two springs and rotates on a shaft fixed on a chassis of the sensor. A hetero-core

optical fiber is clamped at two points, one of which is on the pendulum and the other is fixed on the chassis, thereby the sensor detects the rotation angle of the pendulum as a displacement of the clamped point on the pendulum. When a whole system of the accelerometer was accelerated, the internal pendulum rotates due to an inertial force and makes the position of the clamped point of the hetero-core fiber displaced. Figure 3(b) shows the simplified vibration model of the proposed accelerometer, in which it is supposed that the weight of pendulum exists at a centroid of weight (far from the rotation shaft by L_1 = 25 mm) and is physically subjected to two springs. The effective mass of the weight m_{eff} is determined from the mass of the weight m, those of other components m_i, and the distance of components from the rotation shaft l_i by moment equation as follows:

$$m_{\mathrm{eff}} = m + \frac{1}{L_1}\sum_i m_i l_i, \tag{1}$$

In addition, the effective elastic coefficient k_{eff} is also expressed from k, the elastic coefficient of two employed springs as follows:

$$k_{\mathrm{eff}} = 2k\frac{l_{\mathrm{spr}}}{L_1}, \tag{2}$$

in which l_{spr} denotes the distance of the springs from the rotation shaft. Therefore, when the pendulum is rotated by input acceleration $\alpha(t)$, the equation of motion in the pendulum is described as follows:

$$m_{\mathrm{eff}}L_1\ddot{\theta} + \lambda(\dot{\theta}) + k_{\mathrm{eff}}L_1\theta = m_{\mathrm{eff}}\alpha(t), \tag{3}$$

where θ denotes a rotation angle of the pendulum and λ represents a damping factor of the system including friction around the rotation shaft. From this equation, the resonant frequency of this vibration system f_0 can be derived as follows:

$$f_0 = \frac{1}{2\pi}\sqrt{\frac{k_{\mathrm{eff}}}{m_{\mathrm{eff}}}}. \tag{4}$$

Furthermore, when the frequency of input vibration $\alpha(t)$ is sufficiently lower than the resonant frequency, the following relational expression holds for α and θ because of the first and second terms in the right side of Eq. (3) can be neglected.

$$\frac{d\theta}{d\alpha} = \frac{m_{\mathrm{eff}}}{L_1 k_{\mathrm{eff}}} = \frac{1}{L_1(2\pi f_0)^2}. \tag{5}$$

On the other hand, the hetero-core fiber optic sensor detects the rotation as the displacement $L_2\theta$, when θ is sufficiently small. The relation between the rotation angle θ and an optical loss of the hetero-core sensor is described as follows, on the condition that the sensor linearly responds to the displacement:

$$Loss = \gamma' \mathrm{L}_2\theta = \gamma\theta, \tag{6}$$

in which the coefficient γ means the ratio of optical loss response to the rotation angle. Therefore, considering Eq. (5) and (6), the sensitivity of the accelerometer can be obtained by the following formula:

$$\frac{dLoss}{d\alpha} = \frac{\gamma}{L_1(2\pi f_0)^2}. \tag{7}$$

It can be seen from Eq. (7) that the sensitivity has trade-off relation to the resonant frequency which determines the width of a measurable frequency band, a combination of a weight and springs should be modulated in balance for measuring low-frequency natural vibration in infrastructures with high sensitivity.

3. Static rotation response

For evaluating the sensitivity and linearity of a hetero-core fiber optic sensor to the rotation of pendulum, a static rotation test was conducted, in which the relation between a rotation angle of the pendulum and optical loss response was monitored. As shown in Figure 4, the proposed

accelerometer and a laser displacement sensor measuring the centroid position of the pendulum were fixed on a firm plate rotated by a rotary stage. The rotary stage got the plate slowly inclined by φ in the range of ±8° with a stepwise of 0.5°, and the optical loss and the displacement of weight were simultaneously recorded. In this experiment, two springs inside the accelerometer were removed in advance in order to reduce the difference between the inclination angle φ and the internal rotation angle of pendulum θ. Furthermore, the displacement of weight measured by the laser displacement sensor was regarded as $L_1\theta$ because the rotation angle θ would be sufficiently small.

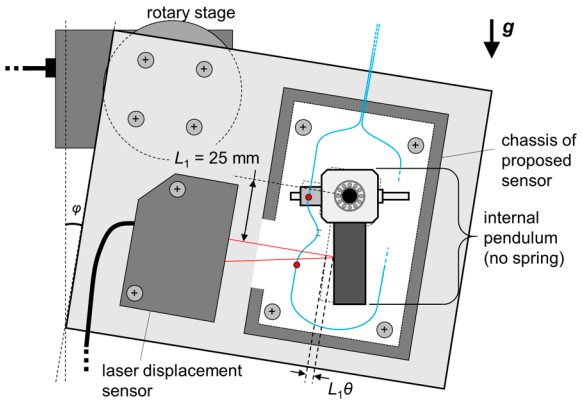

Figure 4. Experimental setup for hetero-core fiber sensitivity to the rotation of a pendulum in the inclined accelerometer.

Figure 5(a) shows the variation of optical loss as a function of the rotation angle of weight θ measured by the laser displacement sensor. It can be seen that the optical loss linearly changed with a sensitivity of 0.0928 dB/° in the range -5° < θ < 5°. In spite of the linear response of a hetero-core fiber optic sensor to the displacement as mentioned in section 2, nonlinear responses in ranges θ < -5° and θ > 5° would result from the change of an axial angle of the optical fiber at a fixed point on the pendulum. In particular, when the pendulum rotated by θ < 0° as depicted in Fig. 5(b.1), θ_{axis}, the axial angle of the optical fiber at a fixed point on the pendulum, was also rotated as much as θ, which made the curvature on the hetero-core portion higher than the case that the only displacement $L_2\theta$ was applied with θ_{axis} = 0°. Similarly in the case θ > 0°, as shown in Fig. 5(b.2), the change of θ_{axis} got lower the increment of curvature on the hetero-core portion due to the applied displacement. Although this phenomenon would always appear in this sensing mechanism, the effect on sensor response appeared to be negligible in the small rotation angle so that the sensitivity of the hetero-core optical fiber to rotation angle γ is 0.0928 dB/° with a linearity in the range of -5° < θ < 5°.

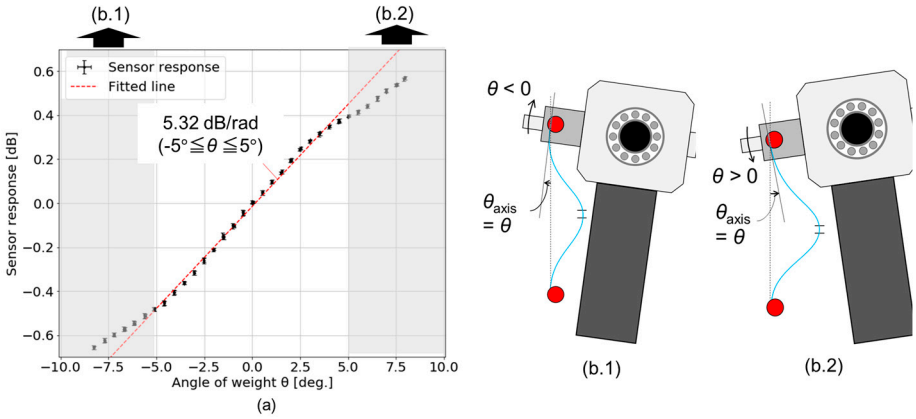

Figure 5. (a) Optical loss variation of a hetero-core optical fiber inside a proposed accelerometer as functions of angle of weight θ, and (b.1) (b.2) schematics of excess changes in the axial angle of the optical fiber line θ_{axis} due to the rotation movement of fixed point on the pendulum.

Preprints (www.preprints.org) | NOT PEER-REVIEWED | Posted: 21 June 2018 doi:10.20944/preprints201806.0335.v1

Peer-reviewed version available at Sensors 2018, 18, 2528; doi:10.3390/s18082528

4. Frequency response characteristics

To understand the optimum specification of the proposed accelerometer for monitoring low-frequency vibration, the frequency responses were monitored with arranging combinations of the weight and springs as listed in table 1. The values of f_0' and $dLoss/d\alpha'$ were calculated as approximate resonant frequencies and sensitivities without considering the effective masses of pendulum components except for a weight. In this experiment, as illustrated in Figure 6, the proposed accelerometer was attached together with an electric accelerometer used as a reference on a stage which was horizontally vibrated by a vibration generator (WaveMaker01, asahi seisakusyo). The waveform applied by the vibration generator was set to be sinusoidal with a frequency ranging from 1 Hz to 50 Hz, and the duration of each test was for 10 seconds in each frequency. During the test, both input acceleration and output data by the reference and the proposed accelerometer were simultaneously measured by a sampling rate of 4 kHz.

Table 1. The combinations m and k of the proposed accelerometer, and approximate values of resonant frequency f_0' and sensitivity $dLoss/d\alpha'$.

Accelerometer	m [kg]	k [N/m]	$f'_0 = \frac{1}{2\pi}\sqrt{\frac{k_{eff}}{m}}$ [Hz]	$\frac{dLoss'}{d\alpha} = \frac{\gamma}{L_1(2\pi f'_0)^2}$ [dB/ms^{-2}]
Pattern 1	0.042	20	3.93	0.349
Pattern 2	0.00644	20	10.0	0.0536
Pattern 3	0.00644	230	34.0	0.00465

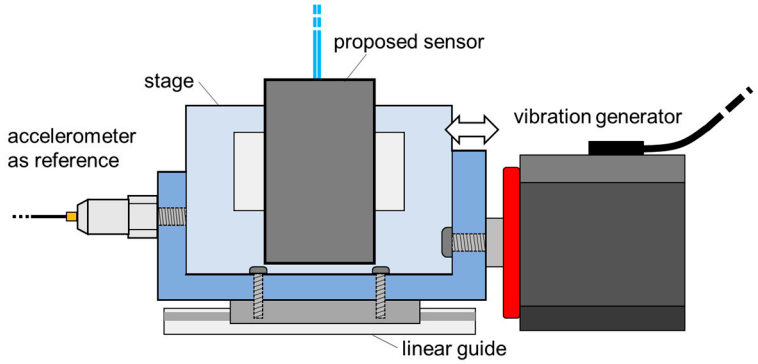

Figure 6. Experimental setup for frequency response characteristics of the proposed accelerometer.

Figure 7 shows the frequency response of the proposed accelerometer, which was obtained as an input-to-output ratio by comparing the amplitudes of the fast Fourier transform (FFT) spectra for each frequency. It was observed that the resonant frequency f_0 shifted with a tendency like f_0' described in table 1, and the sensitivity decreased inversely to the resonant frequency. When calculating $dLoss/d\alpha$ by obtained f_0 according to Eq. (7), the values plotted as dashed lines in Fig. 7 were found to overlap with the measured in frequency bands lower than f_0. In a case of Pattern 1, the input-to-output ratio seems to gradually increase as the increment of frequency. In the other cases of Patterns 2 and 3, however, the stable input-to-output ratios were observed in low-frequency bands up to 4 Hz and up to 15 Hz, respectively.

Additionally, Figure 8 shows profiles of sensor responses in cases of Patterns 2 and 3 when 2- and 4-Hz vibrations were applied. In order not to take into consideration vibrations excited due to resonance, high-frequency components were numerically removed by the finite impulse response (FIR) low-pass filtering with a cut-off frequency of $0.8 \times f_0$. In a case of Pattern 2, it can be seen in Figs. 8(a.1) and (b.1) that the proposed accelerometer responded to vibration with a negligible phase shift comparing to input acceleration data measured by the reference sensor. Moreover, the frequency spectra depicted in Figs. 8(a.2) and (b.2) indicated that the proposed accelerometer well reproduced the frequency spectrum of input acceleration in the range from 1 Hz to the cut-off frequency. There were multiple peaks observed when 2-Hz vibration was applied as shown in Fig. 8(a.2), which were

Preprints (www.preprints.org) | NOT PEER-REVIEWED | Posted: 21 June 2018 doi:10.20944/preprints201806.0335.v1

Peer-reviewed version available at Sensors 2018, 18, 2528; doi:10.3390/s18082528

derived from unwanted harmonic components of input vibration generated by the vibration generator. On the other hand, spectral components under 1 Hz tended to be lower in the sensor response than in input vibration. It would be caused by that the proposed accelerometer had a reduced sensitivity at around 1 Hz, which can be supposed in Fig. 7. These features in terms of a phase shift and a spectral form in a frequency band ranging from 1 Hz to 0.8 × f_0 Hz were similarly observed in the case of Pattern 3 as shown in Figs. 8(c) and (d). As a result, it was confirmed that the proposed accelerometer well performed with a stable sensitivity in a frequency band more than 1 Hz and less than f_0, with keeping the theoretical trade-off relation between the sensitivity and resonant frequency. However, the lower resonant frequency of accelerometer was, the higher but the less stable sensitivity was obtained. For such a reason, the accelerometer should be utilized with moderate adjustments on the internal weight and springs such as in Patterns 2 and 3.

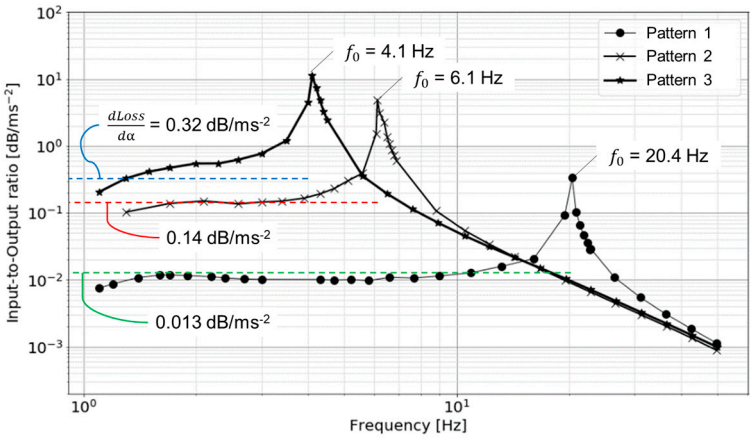

Figure 7. Frequency response characteristics of the proposed accelerometer which was modulated in three patterns shown in table 1.

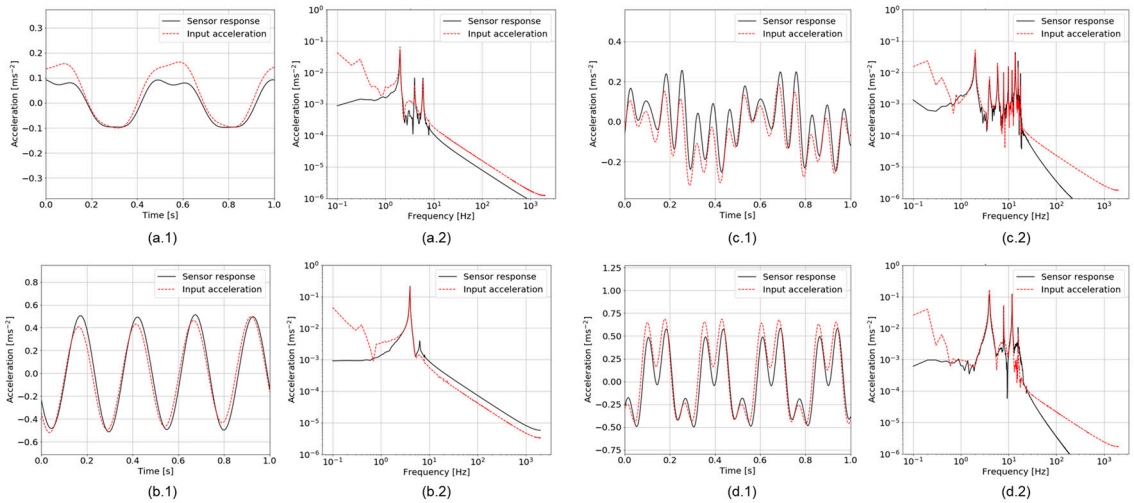

Figure 8. Profiles of responses of the proposed accelerometer and input vibration in (x.1) time domain and (x.2) frequency domain: (a) 2-Hz vibration applied to the proposed accelerometer in pattern 2, (b) 4-Hz vibration to the accelerometer in pattern 2, (c) 2-Hz vibration to the accelerometer in pattern 3, and (d) 4-Hz vibration to the accelerometer in pattern 3.

5. Conclusion

This paper described a novel pendulum-type accelerometer based on hetero-core fiber optics for monitoring low-frequency natural vibrations in large-scale infrastructures such as bridges, building, and tunnels. This accelerometer contained a pendulum with a weight and springs, whose rotation angle was measured by an embedded hetero-core fiber optic sensor. Considering an equation of

motion in the system of pendulum, the rotation angle was proportional to applied acceleration in a range under a resonant frequency.

Through a static rotation test, it was found that the hetero-core fiber sensor linearly responded to the rotation angle in a range within ±5°, although it nonlinearly responded out of this range because the rotation of a fixed point of a fiber line on the pendulum broke the linearity of the sensor response. Moreover, the ratio of rotation angle to applied acceleration varied inversely with respect to the value of resonant frequency f_0, the sensitivity of the accelerometer was able to be calculated from f_0 experimentally observed. Additionally, it was also confirmed that the accelerometer showed a stable sensitivity and reproduced a waveform of input acceleration in a frequency band from 1 Hz to 0.8 × f_0 Hz when the accelerometer was modulated to have f_0 of 6.1 Hz and 20.4 Hz. Consequently, the findings from these experiments have suggested that the proposed accelerometer was suitable for monitoring vibration in a frequency band of several Hz order, and therefore performed well for monitoring low-frequency natural vibrations in large-scale infrastructures.

Author Contributions: Conceptualization, K.W.; Methodology, K.W. and H.Y.; Validation, H.Y. and I.K.; Formal Analysis, H.Y. and I.K.; Investigation, H.Y.; Data Curation, H.Y.; Writing-Original Draft Preparation, H.Y.; Writing-Review & Editing, M.N. and K.W.; Visualization, H.Y.; Supervision, M.N. and K.W.; Project Administration, K.W.

Funding: This work was financially supported by JSPS KAKENHI Grant Number JP18K11363.

Acknowledgments: The work is supported by Core System Japan Co., LTD. The authors appreciate to Joshi Saito, Tetsuya Con, and Hiroyuki Sasaki for their help on sensor development.

Conflicts of Interest: The authors declare no conflict of interest.

References

1. Li, H.-N.; Ren, L.; Jia, Z.-G.; Yi, T.-H.; Li, D.-S. State-of-the-art in structural health monitoring of large and complex civil infrastructures. *Journal of Civil Structural Health Monitoring* **2016**, *6*, 3-16; DOI: 10.1007/s13349-015-0108-9.
2. Salawu, O. Detection of structural damage through changes in frequency: A review. *Engineering structures* **1997**, *19*, 718-723; DOI: 10.1016/S0141-0296(96)00149-6.
3. Sohn, H.; Farrar, C.R. Damage diagnosis using time series analysis of vibration signals. *Smart materials and structures* **2001**, *10*, 446; DOI: 10.1088/0964-1726/10/3/304.
4. Chang, P.C.; Flatau, A.; Liu, S. Health monitoring of civil infrastructure. *Structural health monitoring* **2003**, *2*, 257-267; DOI: 10.1177/1475921703036169.
5. Carden, E.P.; Fanning, P. Vibration based condition monitoring: A review. *Structural health monitoring* **2004**, *3*, 355-377; DOI: 10.1177/1475921704047500.
6. Soman, R.; Kyriakides, M.; Onoufriou, T.; Ostachowicz, W. Numerical evaluation of multi-metric data fusion based structural health monitoring of long span bridge structures. *Structure and Infrastructure Engineering* **2018**, *14*, 673-684; DOI: 10.1080/15732479.2017.1350984.
7. Brownjohn, J.; Koo, K.-Y.; De Battista, N. Sensing solutions for assessing and monitoring bridges. In *Sensor technologies for civil infrastructures*, Elsevier: 2014; pp 207-233; DOI: 10.1533/9781782422433.2.207.
8. Reynders, E.; Wursten, G.; De Roeck, G. Output-only structural health monitoring in changing environmental conditions by means of nonlinear system identification. *Structural Health Monitoring* **2014**, *13*, 82-93; DOI: 10.1177/1475921713502836.
9. Baptista, F.G.; Budoya, D.E.; de Almeida, V.A.; Ulson, J.A.C. An experimental study on the effect of temperature on piezoelectric sensors for impedance-based structural health monitoring. *Sensors* **2014**, *14*, 1208-1227; DOI: 10.3390/s140101208.
10. Dong, B.; Liu, Y.; Qin, L.; Wang, Y.; Fang, Y.; Xing, F.; Chen, X. In-situ structural health monitoring of a reinforced concrete frame embedded with cement-based piezoelectric smart composites. *Research in Nondestructive Evaluation* **2016**, *27*, 216-229; DOI: 10.1080/09349847.2016.1156795.
11. Tibaduiza, D.; Anaya, M.; Forero, E.; Castro, R.; Pozo, F. A sensor fault detection methodology applied to piezoelectric active systems in structural health monitoring applications, In *IOP Conference Series: Materials Science and Engineering*, 2016; IOP Publishing: p. 012016; DOI: 10.1088/1757-899X/138/1/012016.

12. Nguyen, T.; Chan, T.H.; Thambiratnam, D.P.; King, L. Development of a cost-effective and flexible vibration DAQ system for long-term continuous structural health monitoring. *Mechanical Systems and Signal Processing* **2015**, *64*, 313-324; DOI: 10.1016/j.ymssp.2015.04.003.
13. Saleem, H.; Downey, A.; Laflamme, S.; Kollosche, M.; Ubertini, F. Investigation of dynamic properties of a novel capacitive-based sensing skin for nondestructive testing. *Materials Evaluation* **2015**, *73*, 1384-1391; DOI: 10.1088/0957-0233/27/12/124016.
14. Udd, E. Fiber optic smart structures, Society of Photo-Optical Instrumentation Engineers (SPIE) Conference Series, 1993; DOI: 10.1117/12.145196.
15. Minardo, A.; Coscetta, A.; Porcaro, G.; Giannetta, D.; Bernini, R.; Zeni, L. Structural health monitoring in the railway field by fiber-optic sensors. In *Sensors*, Springer: 2015; pp 359-363; DOI: 10.1007/978-3-319-09617-9_63.
16. Hong, C.-Y.; Zhang, Y.-F.; Li, G.-W.; Zhang, M.-X.; Liu, Z.-X. Recent progress of using brillouin distributed fiber optic sensors for geotechnical health monitoring. *Sensors and Actuators A: Physical* **2017**, *258*, 131-145; DOI: 10.1016/j.sna.2017.03.017.
17. Hong, C.-Y.; Zhang, Y.-F.; Zhang, M.-X.; Leung, L.M.G.; Liu, L.-Q. Application of FBG sensors for geotechnical health monitoring, a review of sensor design, implementation methods and packaging techniques. *Sensors and Actuators A: Physical* **2016**, *244*, 184-197; DOI: 10.1016/j.sna.2016.04.033.
18. Fanelli, P.; Biscarini, C.; Jannelli, E.; Ubertini, F.; Ubertini, S. Structural health monitoring of cylindrical bodies under impulsive hydrodynamic loading by distributed FBG strain measurements. *Measurement Science and Technology* **2017**, *28*, 024006; DOI: 10.1088/1361-6501/aa4eac.
19. Yeager, M.; Todd, M.; Gregory, W.; Key, C. Assessment of embedded fiber Bragg gratings for structural health monitoring of composites. *Structural Health Monitoring* **2017**, *16*, 262-275; DOI: 10.1177/1475921716665563.
20. Liu, Q.; Jia, Z.; Fu, H.; Yu, D.; Gao, H.; Qiao, X. Double cantilever beams accelerometer using short fiber Bragg grating for eliminating chirp. *IEEE Sensors Journal* **2016**, *16*, 6611-6616; DOI: 10.1109/JSEN.2016.2588485.
21. Basumallick, N.; Biswas, P.; Dasgupta, K.; Bandyopadhyay, S. Design optimization of fiber Bragg grating accelerometer for maximum sensitivity. *Sensors and Actuators A: Physical* **2013**, *194*, 31-39; DOI: 10.1016/j.sna.2013.01.039.
22. Yang, R.; Bao, H.; Zhang, S.; Ni, K.; Zheng, Y.; Dong, X. Simultaneous measurement of tilt angle and temperature with pendulum-based fiber Bragg grating sensor. *IEEE Sensors Journal* **2015**, *15*, 6381-6384; DOI: 10.1109/JSEN.2015.2458894.
23. Leng, J.; Asundi, A. Structural health monitoring of smart composite materials by using EFPI and FBG sensors. *Sensors and Actuators A: Physical* **2003**, *103*, 330-340; DOI: 10.1016/S0924-4247(02)00429-6.
24. Basumallick, N.; Chatterjee, I.; Biswas, P.; Dasgupta, K.; Bandyopadhyay, S. Fiber Bragg grating accelerometer with enhanced sensitivity. *Sensors and Actuators A: Physical* **2012**, *173*, 108-115; DOI: 10.1016/j.sna.2011.10.026.
25. Liu, B.; Zhong, Z.; Lin, J.; Wang, X.; Liu, L.; Shan, M.; Jin, P. Extrinsic Fabry–Perot Cantilever Accelerometer Based on Micromachined 45° Angled Fiber. *J Lightwave Technol* **2018**, *36*, 2196-2203.
26. Villatoro, J.; Antonio-Lopez, E.; Zubia, J.; Schülzgen, A.; Amezcua-Correa, R. Interferometer based on strongly coupled multi-core optical fiber for accurate vibration sensing. *Optics Express* **2017**, *25*, 25734-25740; DOI: 10.1364/OE.25.025734.
27. Watanabe, K.; Tajima, K.; Kubota, Y. Macrobending characteristics of a hetero-core splice fiber optic sensor for displacement and liquid detection. *IEICE Trans Electron* **2000**, *83*, 309-314; ISSN:0916-8516.
28. Yamazaki, H.; Nishiyama, M.; Watanabe, K.; Sokolov, M. Tactile sensing for object identification based on hetero-core fiber optics. *Sensors and Actuators A: Physical* **2016**, *247*, 98-104; DOI: 10.1016/j.sna.2016.05.032.
29. Sasaki, H.; Kubota, Y.; Watanabe, K. Sensitivity property of a hetero-core-spliced fiber optic displacement sensor, Photonics North 2004: Photonic Applications in Telecommunications, Sensors, Software, and Lasers, International Society for Optics and Photonics: **2004**; pp. 136-144; DOI: 10.1117/12.566868.